The Long-Term Forecast of Station View Periods

M. W. Lo
Mission Design Section

Using dynamical systems theory, a definite integral is obtained that gives the average view period of a ground station for spacecraft in circular orbits. Minor restrictions exist on the class of circular orbits to which this method can be applied. This method avoids the propagation of the orbit, which requires a lot of resources, and simplifies the algorithm used to compute the mean station view period. The integral is used for long-term station load forecast studies. It also provides a quantitative measure of the effectiveness of a ground station as a function of its latitude.

I. Introduction

Planners for the Deep Space Network frequently need to perform long-term station loading studies to determine resource allocations. Typical questions asked by the planners are as follows:

(1) Will the current 34-m subnet be adequate for the support of mission set A for the next 5 years? The mission set represents a collection of current and planned missions that requires support from the subnet.

(2) How will either adding or removing a station at location X affect the performance of the 26-m subnet for the support of mission set B? Will the performance improve if location Y is selected instead of X?

It is important to make the distinction between short-term planning and long-term planning, because the problems encountered are very different. In this article, problems lasting less than a month are defined as short-term planning problems, or scheduling problems; problems lasting more than a month are defined as long-term planning problems, or forecasting problems. The period of 1 month, while somewhat arbitrarily selected, is a convenient demarcation.

With scheduling problems, the interest is in the actual times of events, such as the start and stop times of the view periods of a particular ground station for a set of spacecraft. Typically, the prediction of orbital ephemeris for scheduling activities must be performed weekly or more often due to the various perturbations that cause the actual orbits to quickly drift away from the predicted orbits. Many of the perturbations have random components, and some of the perturbations are not well understood; these factors make their prediction practically impossible. Thus, scheduling problems are concerned with very short durations not far into the future.

With forecasting problems, the interest is not in the actual times of the events but in their long-term trends and cycles. With such problems, the short-term variations are typically ignored due to

their variability and unpredictability. This is usually achieved by averaging techniques; for example, one finds the mean of a parameter by integration over time. Thus, forecasting problems are concerned with long-term trends and average behavior far into the future.

One way to obtain station loading trends is to compute the station view periods, assuming some perturbation models, and then to compute statistics from this database. This has been the method of choice since it is reasonably straightforward to implement. In order to obtain the station view periods, the satellite ephemeris must be propagated. When the period of analysis is 5 to 10 years for a mission set of dozens of spacecraft, this quickly becomes a data-intensive computational problem. For example, using an analytical orbit generator, to compute the view periods of an Earth-orbiting spacecraft with an altitude around 1000 km for the DSN 26-m subnet for the duration of 1 year requires roughly 20 min on a high-speed workstation. For a more complicated orbit generator, with a larger mission set and a longer duration, say 5 years, the time required to generate the view periods alone would be considerable. Thereafter, the large view-period data set requires additional software for manipulation and computation to produce the desired statistics.

Another way to obtain station loading trends is to consider dynamical systems methods. Dynamical systems is the interdisciplinary field that evolved from the qualitative study of differential equations, first begun by Henri Poincaré at the turn of the century. When one sees the adjective \qualitative," one usually assumes no quantitative results can be obtained from such methods. Fortunately, this is not always the case. But the quantities estimated by qualitative methods tend to be global in nature. This article presents an integral that gives the average view period of a spacecraft to a ground station and is derived using dynamical systems theory[1].

II. The Long-Term Station View Period Ratio, r

An integral was obtained that represents the long-term station view period ratio, ρ, for the class of circular orbits with nonrepeating ground tracks. This ratio provides an estimate of the total time a station is in view of a spacecraft divided by the total elapsed time. More precisely, let

T = total elapsed time

$P(T)$ = total station view period during the elapsed time T

then the long-term station view period ratio is defined by

$$\rho = \lim_{T \to \infty} \frac{P(T)}{T} \tag{1}$$

Thus, given a time period, T, the total amount of time a station is in view of the satellite is given by the following expression:

$$V(T) = \rho T \tag{2}$$

As the ratio, ρ, is a limit, the larger the value of T, the closer $P(T)$ is to $V(T)$. For example, for a 200-km circular orbit with an inclination of 28.5 deg (Case 1, Table 1), the total view period at a ground station at 0-deg latitude for 1 year as computed by $P(T)$ and $V(T)$ is

$$P(1 \text{ year}) = 0.021014 \text{ year}$$

$$V(1 \text{ year}) = 0.021030 \text{ year}$$

[1] An article describing the full derivation of the integral is under preparation.

Here $P(T)$ is computed by propagating the orbit and finding all of the view periods of the station at latitude 0 deg; $V(T)$ is computed from Eq. (2), where the ratio, η is given by the integral.

Preliminary numerical results indicate excellent agreement between the numerical and the theoretical values for the view period ratio, η for circular orbits. The numerical values are computed typically from 1 year's worth of station view periods. For the circular orbits used in the numerical study, $\Delta\eta$ is less than ± 0.2 percent, where $\Delta\eta$ is the difference between the theoretical and numerical values of η. For the elliptic orbits used in the numerical study, at $e = 0.05$, the maximum $\Delta\eta$ for the cases tested exceeds 15 percent. For orbits whose period is commensurate with the Earth's rotational period, the $\Delta\eta$ for the cases tested is within ± 1.5 percent. These results are tabulated in Tables 1 through 3 and discussed in Section V.

III. Heuristics and Theoretical Background

Examine first the geometry of the spacecraft and the ground station. Figure 1 shows the geometry of the station mask, which is determined by the altitude of the spacecraft and has the following interpretation. The station mask is the circle of angular radius, μ_0, about the ground station. When the spacecraft ground track is within the station mask, the spacecraft is in view of the station. When the ground track is outside of the station mask, the spacecraft is not in view of the station. The angle ε, is the minimum station elevation angle below which the station cannot view the spacecraft, due to some constraint or obstruction at the horizon. In particular, when the spacecraft-to-station elevation angle is ≤ 0 deg, then the Earth itself is obstructing the spacecraft from the station view. A spherical Earth is assumed here.

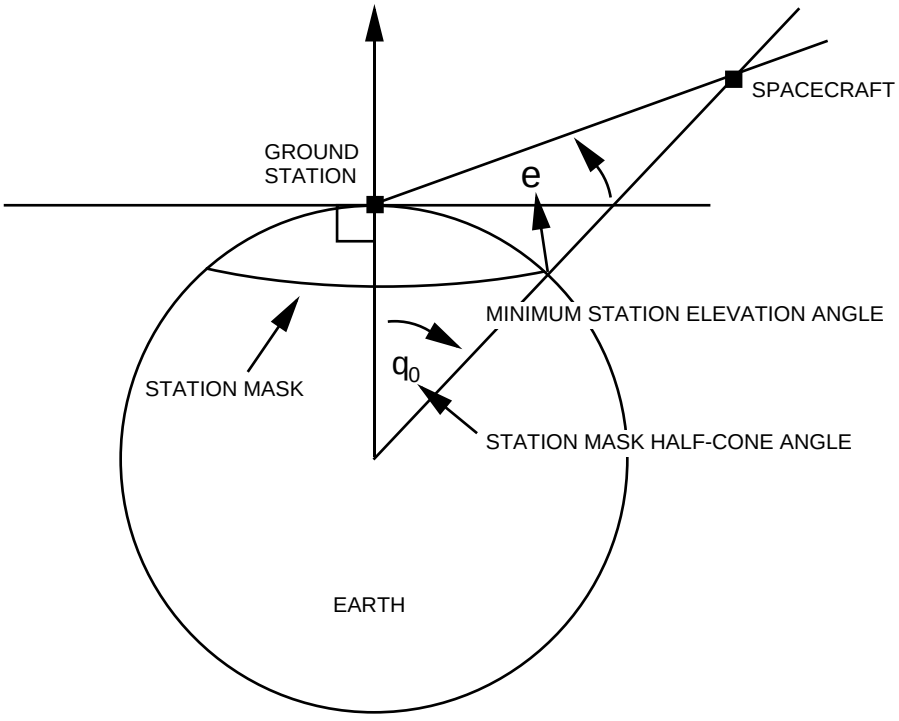

Fig. 1 Geometry of the station mask.

Figure 2 illustrates the ground tracks of a spacecraft in circular orbit at a 7714.14-km radius (this is the radius of the TOPEX/POSEIDON orbit) and a 28.5-deg inclination. The circle centered at the equator with the label "Case 4" is the station mask of a fictitious station on an ocean platform at the equator (latitude = 0 deg) with longitude equal to that of the 26-m station at Goldstone. The station

mask of the Madrid station is labeled \Case 7" and that of the Canberra station is labeled \Case 6." They are only partially in view. Consider a station at the pole; its mask is the cap about the pole. For the spacecraft in Case 4, this cap does not intersect the ground track pattern. This means that the spacecraft would not see the station at the pole. The Madrid station mask (Case 7) intersects the ground tracks in a much smaller area than that of Case 4. Intuitively, one might think that, somehow, the total view period (sum of all the view periods) is proportional to the area of the intersection between the band of the ground track and the station mask. After all, when there is no intersection, there is no view period. When there is a lot of intersection, there is a large view period. But, unfortunately, this is not the whole story. There are other factors.

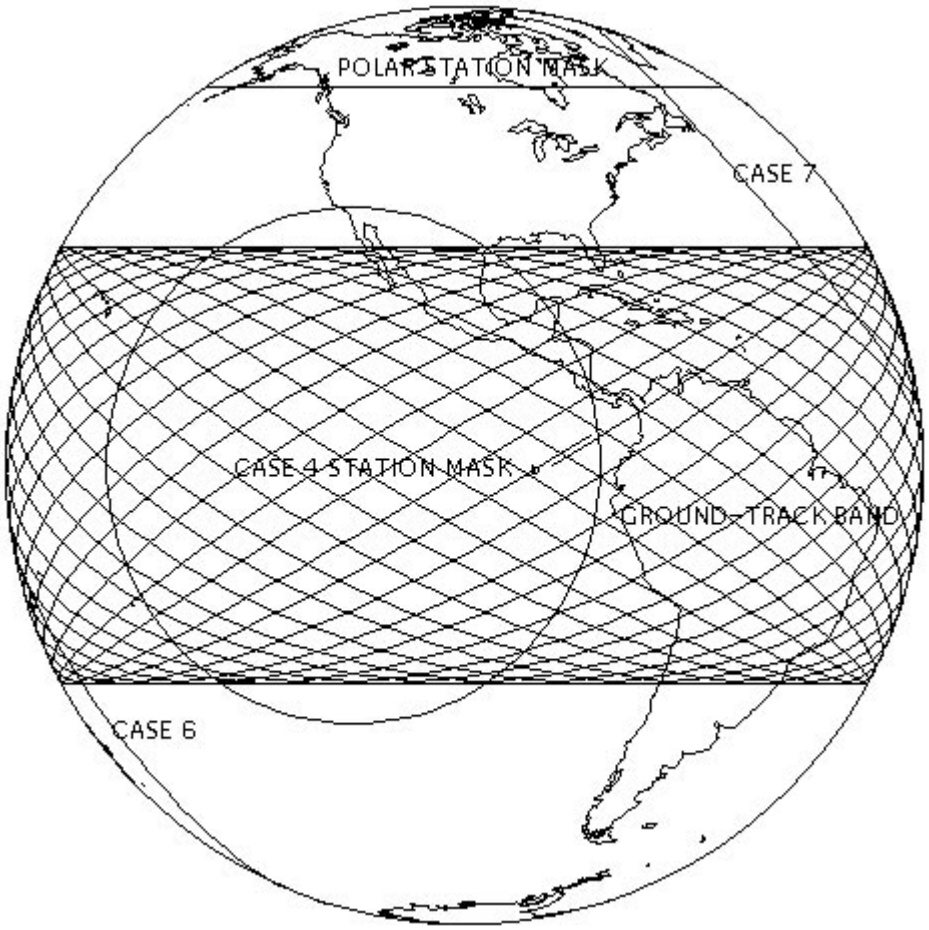

Fig. 2. Station masks and ground tracks for cases 4, 6, and 7 (orthographic projection).

Consider the following example: suppose now that the orbit is of su±ciently high inclination and low altitude that the station mask is a small circle completely within the ground track band, as illustrated in Fig. 3. Calculations quickly show that Station 1 has a much higher total view period than Station 2, even though they have the same mask area and are both enveloped by the spacecraft ground tracks. This agrees with the well-known observation that stations at higher latitudes tend to have more and longer view periods.

This problem is resolved by looking at Fig. 2 more carefully. Notice that the ground tracks are more closely packed near the top than near the equator. Furthermore, the speed of the spacecraft nadir along the ground track is not constant even though that of the circular orbit is constant. This is due to the

rotation of the Earth and the projection of the spacecraft motion onto the sphere. Thus, the time spent near the equator and that near the top and bottom of the ground track band is not the same. However, the station mask is una®ected by the rotation of the Earth, and it has the same size regardless of the location of the station. Hence, going back to Fig. 3, even though the two station masks contain the same amount of ground track area, the actual time spent in each area is not the same. Thus, one has to use a weight factor to compute the area of intersection in order for it to be proportional to the total view period. In mathematical terms, one needs to ¯nd an invariant measure for the dynamics. This measure will give the connection between the weighted area of the mask and the time spent in the mask. This has been done for the case of circular orbits with certain mild restrictions and is discussed in the next section.

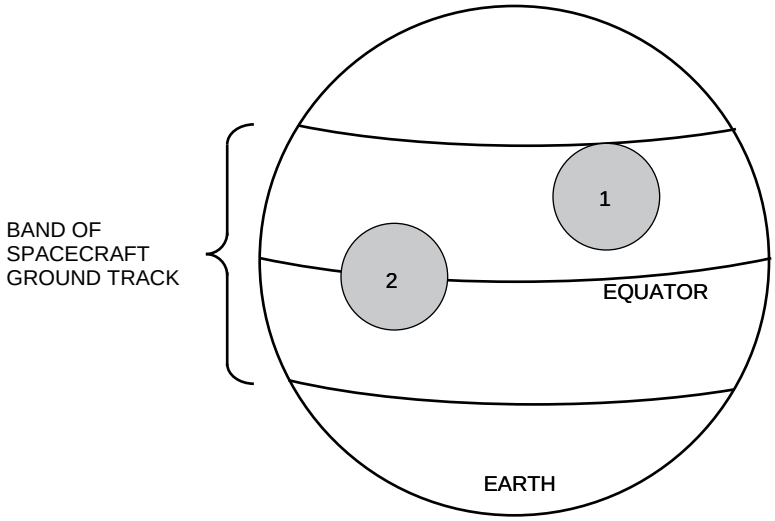

Fig. 3. Station masks at different latitudes.

The system of spacecraft ground tracks belongs to a class of dynamical systems known as \ergodic." The discussion on ergodic theory below drew on [1{3]. The analysis used many of the ideas described in [4]. The important property about ergodic systems for this discussion is the following.

Let $F(x)$ be a well-behaved function on the space where there is an ergodic system. Then the time mean of F and the space mean of F are equal. The time mean of F is the path integral of $F(x)$ along the trajectory as a function of time. The space mean of F is simply the integral of F over the space. This is known as the Ergodic Theorem.

Now let F be the station view function. This means F is equal to 1 when the spacecraft is in view of the station, and F is equal to 0 otherwise. The time mean of F is just the time average of the total view period. The view periods require a lot of calculations, which one would like to avoid. But the Ergodic Theorem states that one can skip all this computation by simply calculating the space mean of F. This is a great simpli¯cation; notice that the space mean of F is just its integral over the sphere, which is easy to compute. One arrives at the following:

$$\lim_{T \to \infty} \frac{P(T)}{T} = \text{time mean of } F$$

$$\int_{EARTH} F(x)\,d\mu = \text{space mean of } F$$

$$\nu = \lim_{T \to \infty} \frac{P(T)}{T} = \int_{EARTH} F(x)\, d\mu$$

The construction of the weight function, μ, also known as the invariant measure, is geometric in nature. Referring back to Fig. 2, follow a small segment along the ground tracks and see how it gets stretched as time progresses. This stretching factor then enables one to compute μ. It is this weight function that enables one to relate the time with the area. Having done so, it becomes an easy task to perform the integral, F, whereupon, one has computed the long-term view period ratio ν. This demonstrates the power of qualitative methods even for engineering applications.

IV. The Integral Representation of ν

The integral ν for a spacecraft in circular orbit is subject to the following perturbations and constraints:

(1) The spacecraft is in circular orbit; the orbit eccentricity is 0.

(2) The spacecraft is perturbed only by the linear J_2 term of the spherical harmonic expansion of the gravity field of Earth. Thus, the first-order linear perturbations for the node and argument of perigee are:

$$\Omega(T) = \Omega_0 + \frac{d\Omega}{dt} T$$

$$\omega(T) = \omega_0 + \frac{d\omega}{dt} T$$

The derivatives $d\Omega/dt$ and $d\omega/dt$ are constant. The semimajor axis, eccentricity, and inclination are constant. Mean elements are assumed throughout this discussion.

(3) The orbit inclination is not 0 deg. Circular orbits with a 0-deg inclination have constant view periods that can be easily calculated[2].

(4) The orbit has an orbital period that is incommensurate with the period of the Earth's rotation. Hence, this orbit does not have repeating ground tracks.

(5) The ground station is not centered at the north or south pole.

(6) The intersection of the station mask with the ground-track region forms a simply connected domain.

The variables and the integral for ν are

$$\left.\begin{aligned} \nu &= \text{long-term station view period ratio} \\ \theta_0 &= \text{station latitude } \theta \neq \pm 90 \text{ deg} \\ \mu_0 &= \text{station mask angular radius} \\ &= \arccos(R_E/R) \text{ for stations with } \varepsilon = 0 \text{ deg} \\ R_E &= \text{Earth radius} \\ R &= \text{spacecraft orbit radius} \\ \varepsilon &= \text{minimum station elevation angle} \end{aligned}\right\} \quad (3a)$$

[2] M. W. Lo, "The View Period of Circular Equatorial Orbits," JPL Interoffice Memorandum 312/94.7-10 (internal document), Jet Propulsion Laboratory, Pasadena, California, June 3, 1994.

$$
\left.
\begin{aligned}
i &= \text{spacecraft orbit inclination} \quad > 0 \text{ deg} \\
L_i &= \begin{cases} i & \text{if } i \le 90 \text{ deg} \\ 180^\circ - i & \text{if } i > 90 \text{ deg} \end{cases} \\
\psi_1 &= \max\left[\psi_0 - \mu_0, L_i\right] \\
\psi_2 &= \min\left[\psi_0 + \mu_0, L_i\right] \\
f(\psi) &= \frac{\cos\psi}{\left[1 - \sin^2 i - \sin^2\psi\right]^{1/2}} \\
\theta &= \int_{\psi_1}^{\psi_2} f(\psi)\, d\psi
\end{aligned}
\right\} \qquad \text{(3b)}
$$

V. Numerical Verification

Three sets of tests were performed to verify the algorithm. The first set used circular orbits; the results are shown in Table 1. The second set used elliptic orbits with eccentricity = 0.05; the results are shown in Table 2. The third set used orbits with repeating ground tracks; the results are shown in Table 3. The parameter that measures the accuracy of the model is ϵ_θ (listed in the last column of the tables):

$$
\epsilon_\theta\,\% = 100\,\frac{\theta_{\text{THEORY}} - \theta_{\text{NUMERIC}}}{\theta_{\text{NUMERIC}}}
$$

Table 1 lists the 31 cases used in the verification of Eq. (3). The numerical view periods are generated by propagating the orbit using the linear J_2 perturbations. The integral for θ is evaluated using a mathematical symbolic computation program. The low Earth orbits selected for the verification have various altitudes with inclinations at 28.5, 48, 88.5, 98.5, and 151.5 deg. For those cases with an asterisk in front of the inclination, the orbit propagation begins at the descending node. For all other cases, the orbit propagation begins at the ascending node. The cases in Table 3 use an orbit with repeating ground tracks with a repeat pattern of 20 orbits in 3 days. All other orbits have nonrepeating ground tracks; thus, their periods are incommensurate with that of the period of the Earth's rotation.

The stations at latitudes of 0, 5, and 10 deg have the longitude of the 24-m Goldstone DSN station. The stations at latitudes of −35.4 and 40.4 deg are the 24-m Canberra and Madrid DSN stations, respectively.

The ϵ_θ for the circular orbits of Table 1 are plotted in Fig. 4. It shows the differences between the theoretical and numerical values of θ for these orbits to be under 0.2 percent, indicating excellent agreement.

Figure 5 plots the ϵ_θ of the circular orbits from Table 1 as a solid curve on top of which the values for the corresponding elliptic orbits from Table 2 have been added. For example, Case E1 and Case 4 in Fig. 5 have the same test parameters except for the orbit eccentricity. By changing the eccentricity of the orbit of Case 4 to 0.05 while keeping all other parameters fixed, ϵ_θ increased from under 0.2 percent to about 1 percent. But for Case 23, the change in eccentricity and the high inclination caused ϵ_θ to exceed 15 percent. This shows that the algorithm does not work as well for elliptic orbits. However, the accuracy may be sufficient for load studies since many of the parameters are even less well known.

Figure 6 plots the ϵ_θ of orbits with repeating ground tracks from Table 3; a single fixed orbit with a repeat pattern of 20 orbits in 3 days is used with different stations for these cases. The difference between the theoretical and numerical values of θ is still quite good at less than 1.3 percent.

Table 1. Comparison of numerical versus theoretical long-term view period ratio for circular orbits with nonrepeating ground tracks (eccentricity = 0).

Case number [a]	Orbit radius, km	Orbit inclination, deg [b]	Station latitude [c]	Numeric [d]	Theory [e]	Di®erence [f]	Percentage [g]
1	6578.14	28.5	0.0	0.021014	0.021030	0.000015	0.072847
2	6578.14	28.5	¡ 35.4	0.014719	0.014740	0.000020	0.138198
3	6578.14	28.5	40.4	0.004976	0.004985	0.000009	0.178944
4	7714.14	28.5	0.0	0.154513	0.154505	¡ 0.000008	¡ 0.005178
5	7714.14	28.5	5.0	0.148701	0.148664	¡ 0.000037	¡ 0.024882
6	7714.14	28.5	¡ 35.4	0.085387	0.085383	¡ 0.000004	¡ 0.004685
7	7714.14	28.5	40.4	0.073382	0.073393	0.000011	0.014854
8	7714.14	*28.5	0.0	0.154513	0.154505	¡ 0.000008	¡ 0.005178
9	7714.14	*28.5	¡ 35.4	0.085368	0.085383	0.000015	0.017454
10	7714.14	*151.5	0.0	0.154543	0.154505	¡ 0.000038	¡ 0.024589
11	7714.14	*151.5	¡ 35.4	0.085507	0.085383	¡ 0.000124	¡ 0.145017
12	7714.14	*151.5	40.4	0.073483	0.073393	¡ 0.00009	¡ 0.122614
13	7714.14	151.5	5.0	0.148658	0.148664	0.000006	0.004036
14	7714.14	151.5	¡ 35.4	0.085361	0.085383	0.000022	0.025421
15	7714.14	151.5	40.4	0.073422	0.073393	¡ 0.000029	¡ 0.039498
16	7714.14	48.0	0.0	0.081425	0.081432	0.000007	0.008351
17	7714.14	48.0	5.0	0.082509	0.082453	¡ 0.000056	¡ 0.067993
18	7714.14	48.0	10.0	0.086041	0.086012	¡ 0.000029	¡ 0.033821
19	7714.14	48.0	¡ 35.4	0.100203	0.100189	¡ 0.000014	¡ 0.013972
20	7714.14	48.0	40.4	0.096789	0.0968	0.000011	0.011675
21	7714.14	61.0	0.0	0.067089	0.067078	¡ 0.000011	¡ 0.016424
22	7714.14	61.0	¡ 35.4	0.099756	0.099737	¡ 0.000019	¡ 0.018588
23	7714.14	61.0	40.4	0.102233	0.102237	0.000004	0.003912
24	7714.14	88.5	0.0	0.057763	0.057726	¡ 0.000037	¡ 0.064401
25	7714.14	88.5	¡ 35.4	0.072831	0.07285	0.000019	0.025538
26	7714.14	88.5	40.4	0.079102	0.079127	0.000025	0.031731
27	7714.14	98.5	0.0	0.05849	0.058413	¡ 0.000077	¡ 0.132331
28	7714.14	98.5	¡ 35.4	0.074554	0.074609	0.000055	0.073638
29	7714.14	98.5	40.4	0.081762	0.081743	¡ 0.000019	¡ 0.02385
30	10,000.14	61.0	0.0	0.15332	0.153309	¡ 0.000011	¡ 0.007175
31	10,000.14	61.0	5.0	0.155375	0.155142	¡ 0.000233	¡ 0.14996

[a] Circular orbits. All orbits have nonrepeating ground tracks.
[b] The * indicates the orbit propagation started at the descending node. All other cases started at the ascending node.
[c] The stations with latitudes at 0, 5, and 10 deg have the longitude of the Goldstone station. The station with latitude at ¡ 35.4 deg is the Canberra station. The station with latitude at 40.4 deg is the Madrid station.
[d] (Total view periods)/(total time), numerically generated using linear J_2 orbit propagation.
[e] Limit (total view periods)/(total time), theoretical value.
[f] Theory ¡ numeric.
[g] (Di®erence/numeric) £ 100.

Table

s theoretical long-term view p
eccentricity = 0.05).

Orbit radius km	Numeric [d]	Theory [e]	Di
714	0.152476	0.154505	
14	0.086059	0.085383	¡ 0
4	0.072582	0.073393	0
4	0.067196	0.067078	¡ 0.
	0.112791	0.099737	¡ 0.
	0.088053	0.102237	0
	0.057875	0.057726	¡ 0.
	0.071308	0.072850	0.
	0.081627	0.079127	¡ 0.
	0.261715	0.261864	0.
	0.173428	0.173361	¡ 0.0
	0.158665	0.158644	¡ 0.0
	0.153501	0.153308	¡ 0.0
	19271	0.18373	¡ 0.0
	17489	0.184627	0.0

s.

ngitude of the Goldstone st
ation. The station with latitu

ed inear J_2 orbit propag
e.